

Numerical simulation of peel test for ductile thin film along ceramic substrate: Elasto-plastic analysis

A. Adjeloua^{1,*}, N. Boualem¹, H. Meddah² and A. Belarbi²

¹ Laboratory of Composites Structures and Innovative Materials (LCSIM), Mechanical Engineering Faculty, USTO MB Oran BP 1505 EI- M'Naouar, Oran, Algeria

² Department of Mechanical Engineering, USTO MB Oran BP 1505 EI M'Naouar, Oran, Algeria

ABSTRACT – Due to extensive applications of the thin film/substrate systems in engineering, the research on strength, ductility and reliability of these systems have attracted great deal of interest in recent years. The peel angle of debonded film on the ceramic substrate has a very important effect in the mechanical resistance of film/substrate bi-material. Among critical debonding parameters, peeling angle and thermal residual stresses can be a potential risk of brutal propagation causing the film/substrate composite failure under tensile loading. This study is carried out to analyze the peeling angle and residual thermal stresses effects with crack growth in the specimen. A two dimensional elastic-plastic finite element model is used to compute the J-integral and estimate the plastic zone size at the interfacial crack tip of film/substrate composite. Results show that the peeling phenomena is a fracture mixed mode where the dominance of either mode I or mode II is influenced by the peeling angle while delamination of thin film is greatly dependent on thermal residual stresses.

ARTICLE HISTORY

Received: 22nd Oct 2019

Revised: 18th Aug 2020

Accepted: 08th Sept 2020

KEYWORDS

Finite element method;
film;
substrate;
J-integral;
plastic zone

INTRODUCTION

Several application fields related to thin films and their film/substrate adherence capability are of great interest [1-3]; however, delamination can occur for various reasons such as residual and thermal stresses and the difference in expansion coefficient of the film/substrate pair. In the classical peel test, the energy dissipated by mechanisms other than delamination should be accounted [4-6] to determine intrinsic interface properties where the local mode mixity is evaluated based on analytical results. A semi-analytical expression for the work done by bending plasticity is proposed to provide a precise value of the interface fracture energy [7]. A trans-scale mechanics model has been adopted to describe the interfacial fracture behaviors of the metal thin film peeled on the ceramic substrate and optimization scheme for peel force and root rotation [8, 9]. In the nonlinear delamination analysis for thin films using conventional elastic-plastic theory, results show that the peak separation stress levels during the delamination of the film can never exceed 4 times the yield stress [10, 11]. Wei and Hutchinson [12] presented a steady-state delamination study of an elastic film on an elastoplastic substrate or an elastoplastic film on an elastic substrate under uniform equi-biaxial stress, using the embedded process zone fracture model (EPZ) [13, 14]. Suo et al. examined a plasticity-free strip with (SSV) model [15]. Peel test is one of the most important methods to evaluate the interface mechanical properties, mainly to determine the interface properties between films and substrates. Due to its importance, the peel test has been widely applied in many research areas [16-18]. However when thin film or substrate is a ductile material, the measured peeling force is often much larger than the interfacial adhesion toughness. The phenomenon arises from the plastic dissipation due to material plastic loading and unloading deformation. In order to model the increase of peeling force (or energy release rate) due to plastic dissipation, Thouless and Yang [19] carried out a two-dimensional finite-element analysis of the peel test in which a cohesive-zone model is adopted for the peeling of an elastic-plastic film while Ghabezi and Farahani [20] studied the cohesive mechanism and traction-separation parameters in mode I and II fracture. They showed that the peel force depend on the toughness of the interface and by crack-tip plasticity induced by the cohesive stresses.

In the previous following decade, various investigations related to delamination of ductile thin film adopting a bending model was presented [21-23]. Chauffaille et al. [24] carried out an elastoplastic analysis of a single cantilever beam (SCB) adhesion test, in which only the thin film is subjected to applied bending moment sufficiently great to induce elastoplastic behaviour in the assumed adherend. However, Zhang and Wang [25] adopted a cohesive zone model to analyze the elastic-plastic thin film peeling problems using the energy of adhesion and the peak separation stress as key parameters called interface strength. The strain gradient incremental theory has been developed and used to study the steady-state crack growth in mode I [26, 27]. The result shows that the peak interface separation stress ahead of crack tip can reach a value over ten times the material yielding stress.

The presence of residual stress field in thin film/substrate has a strong effect on their performances and plays a major role in this composite failure behaviour. In general, the residual stress state in a thin film is complicated, depending on fabrication process specifics and varying through the film thickness [28-33]. From the literature presented, which is by

no means an exhaustive list, it is clear that there are considerable efforts dedicated to modeling, understanding and explaining peeling phenomenon. However, existing models have many shortcomings due to the intrinsic complexity of adhesion system. One of the debonding aspects that has not yet been fully explored is the dissipated energy rate based J-integral method computing all stress and strain fields around the crack tip located between elastic rigid substrate and elastoplastic film.

In this study, finite element method (FEM) is used to investigate the peeling behaviour of an elastic-plastic film bonded on an elastic substrate using J-integral concept to evaluate the energy rate in the vicinity of the crack tip located at the interface. The plastically deformed region of the peel was estimated to quantify the part of energy dissipated in this process zone. Also peeling angle, crack length and thermal residual stresses were highlighted.

GEOMETRICAL AND NUMERICAL MODEL

Figure 1 illustrates a 2D geometrical model carried out with Abaqus software [34]. The composite consists of two dissimilar materials fully bonded: alumina (substrate) and aluminum film, characterized by their mechanical properties; Young moduli $E_s = 345$ GPa and $E_f = 72$ GPa, Poisson ratio $\nu_s = 0.3$ and $\nu_f = 0.3$ while h_s and h_f indicate the thickness (s and f subscripts are related to substrate and film respectively) and b is the width of the specimen. Thickness and stiffness of the substrate are generally much greater than those of the film. An edge interface crack of length a is considered. The film is subjected to a tensile load $F = \sigma_0 \cdot b \cdot h_f = P \cdot b$ ($\sigma_0 = 40$ MPa) and the substrate bottom edge is fixed.

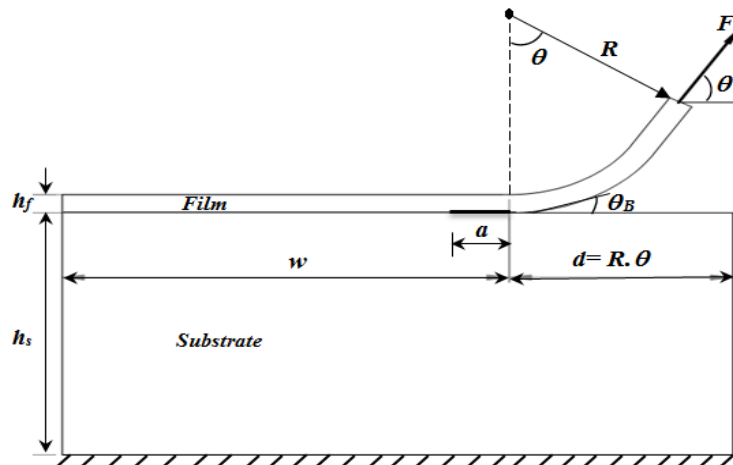


Figure 1. Geometrical model of film bonded to a substrate

Figure 2 shows the meshed specimen with a refined mesh near the contact region and a gradually coarse mesh further from the contact region to ensure numerical accuracy. The composite film/substrate is modeled using 36750 elements, the crack tip region is modeled by eight noded (CPS8R) and the quarter-point elements, as shown in Figure 2(b) allowing to relieve the singularity problem when assessing the integral J which is also independent of the integration path while the remaining area is meshed with triangular elements (CPS6M), Figure 2(a).

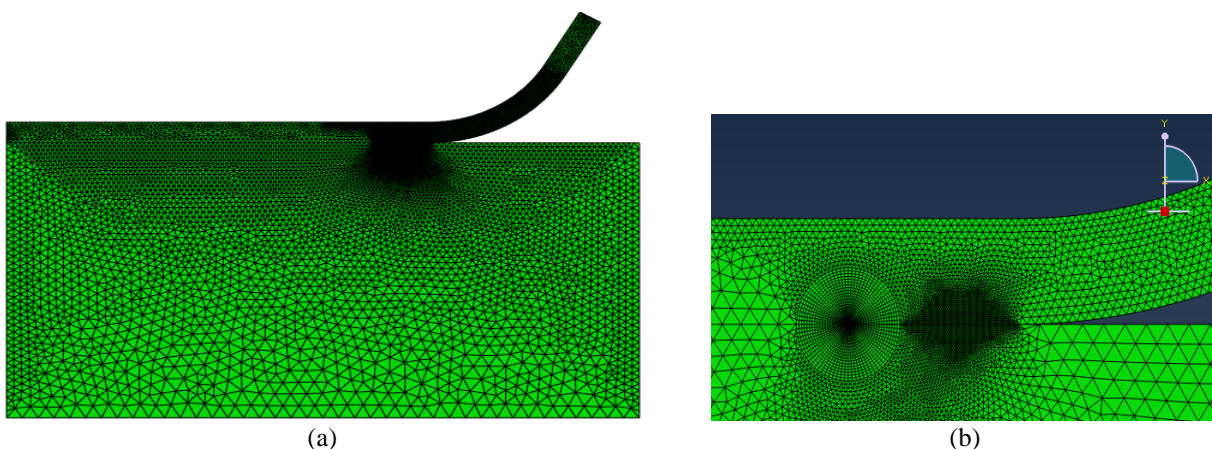


Figure 2. Typical mesh model of film bonded to a substrate: (a) full mesh and (b) detailed mesh

The behaviour of substrate (Ceramic) very rigid is considered to be linear elastic and the film (Aluminum) to exhibit an elastic plastic constitutive behaviour whose plastic part obeys a power law in $\sigma = \sigma_y (\epsilon/\epsilon_y)^m$ form with yielding stress $\sigma_y = 350$ MPa and an exponent $m = 0.1315$ as represented in Figure 3. The FEM simulations with non linear analysis using automatic time stepping are carried out using ABAQUS code.

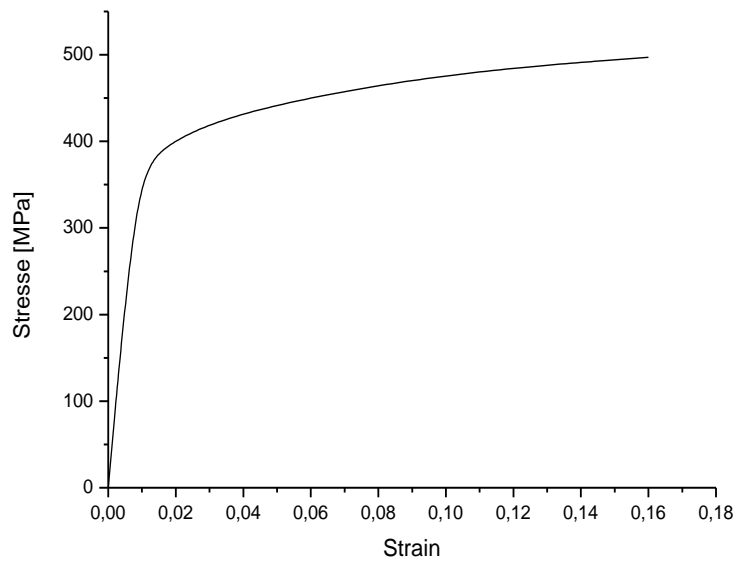


Figure 3. Stress–strain curve of film

RESULTS AND DISCUSSION

Energy Balance

An energy balance is often used to relate the determined peel force to the specific fracture energy. In this specimen, the peel arm is assumed as a part of circle with a crack termination at the root. The applied force F to the adherend is inclined by an angle θ relative to the horizontal axis. During elastic peeling, part of the work done by the peel force is stored in the elastically deforming system and the rest is used to provide the work required to break the interfacial bonding and create the new fracture surface with a crack length a . When plastic dissipation occurs around the crack tip due to singular strains, bending is the predominant mode of delamination during plastically deforming film. By superposition principle, the above model in Figure 1 can be decomposed in two parts as shown in Figure 4.

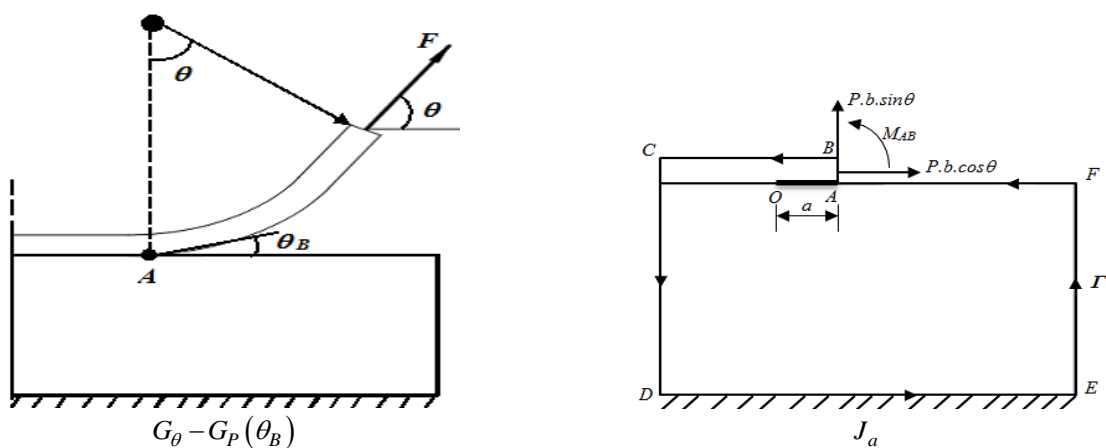


Figure 4. Equivalent model

with,
$$M_{AB} = P.b.\sin \theta.R.\sin \theta - P.b.\cos \theta.R.(1 - \cos \theta)$$

which becomes,
$$M_{AB} = P.b.R.(1 - \cos \theta)$$

Therefore, in a stress state elastic plastic peeling the energy balance can be written as:

$$J = G_\theta - G_p(\theta_B) + J_a \tag{1}$$

$$G_\theta = \frac{F}{b}(1 - \cos \theta) = P(1 - \cos \theta) \quad \text{is the energy release rate where} \quad P = \frac{F}{b}$$

$$G_p(\theta_B) = G_p(k_B) = \frac{3P}{\eta} f_i(k_B) \quad \text{is the plastic dissipation rate where} \quad \eta = \frac{6E_f P}{h_f \sigma_y^2} \quad \text{is the normalized force and}$$

$k_B = [\eta(1 - \cos \theta_B)]^{1/2}$ is the maximum curvature at the base angle θ_B .

$$f_i(k_B) = \begin{cases} f_1(k_B) = 0 & \text{for } 0 < k_B < 1 \\ f_2(k_B) = \frac{3}{\eta} \left(k_B - \frac{7}{4} + \frac{1}{3k_B} + \frac{1}{2k_B^2} - \frac{1}{3k_B^4} \right) & \text{for } 1 < k_B < 2 \\ f_3(k_B) = \frac{3}{\eta} \left(2k_B - \frac{23}{4} + \frac{10}{3k_B} + \frac{7}{2k_B^2} - \frac{49}{3k_B^4} \right) & \text{for } k_B > 2 \end{cases} \tag{2}$$

Case 1: For $0 < k_B < 1$ peeling involves only elastic bending, i.e. no plastic dissipation is involved $G_p = 0$.

Case 2: For $1 < k_B < 2$ peeling involves elastic-plastic loading and elastic unloading, but no reverse plasticity.

Case 3: For $k_B > 2$ reverse plastic deformation is involved.

$$J_a = \int_\Gamma \left(W dy - T_i \frac{\partial U_i}{\partial x} ds \right)$$

is the J-integral part due to the presence of the crack a . For this purpose an independent path contour Γ is chosen as shown in Figure 4; $W = \sigma_{ij} \epsilon_{ij}$ is the strain energy density, $T_i = \sigma_{ij} n_j$ the traction vector along the

contour Γ , $\frac{\partial U_i}{\partial x} = \frac{\partial}{\partial x} \begin{pmatrix} u \\ v \end{pmatrix}$ is the derivative of the displacement vector and ds denotes an increment along the contour Γ .

The J-integral on all parts of Γ is vanished by both or either $\sigma_{ij} = 0$ and $dy = 0$ excepted the edge AB where its value is obtained by integration along the elastic and plastic zones, i.e.

$$J_a = J_{el} + J_{pl} \tag{3}$$

According to [35] and setting $h_f = h$ and $E_f = E$, the J-integral is equal to:

$$J_a = \underbrace{\frac{M}{2bh^3} \kappa h_{el}^3}_{el} + \underbrace{\frac{\sigma_y^2}{E} \frac{1-m}{m+1} \left(\frac{h}{2} - \frac{h_{el}}{2} \right) + \frac{m}{(m+1)(m+2)2^{m+1}} E^m \sigma_y^{1-m} \kappa^{m+1} (h^{m+2} - h_{el}^{m+2})}_{pl} \tag{4}$$

where, $M = (P.b.a.\sin \theta + M_{AB})$

$$\kappa = \frac{1}{\rho} = \frac{M}{EI}$$

is the curvature of segment OA under bending determined from the following equation:

$$\kappa^{2+m} + c\kappa^2 + d = 0$$

$$c = -\frac{2^{m+1}(m+2)M\sigma_y^{m-1}}{bh^{2+m}E^{2+m}}$$

$$d = \frac{4(m-2)2^m\sigma_y^{2+m}}{3h^{2+m}E^{2+m}}$$

With,

and $I = I_z = \frac{bh^3}{12}$ is the moment of inertia of the cross-section AB.

m is the exponent of the power law $\sigma = \sigma_y (\epsilon/\epsilon_y)^m$, h_{el} is the height of the elastic zone in the cross-section AB obtained from the equation $h_{el} = \frac{2\sigma_y}{E\kappa}$ as shown in Figure 5.

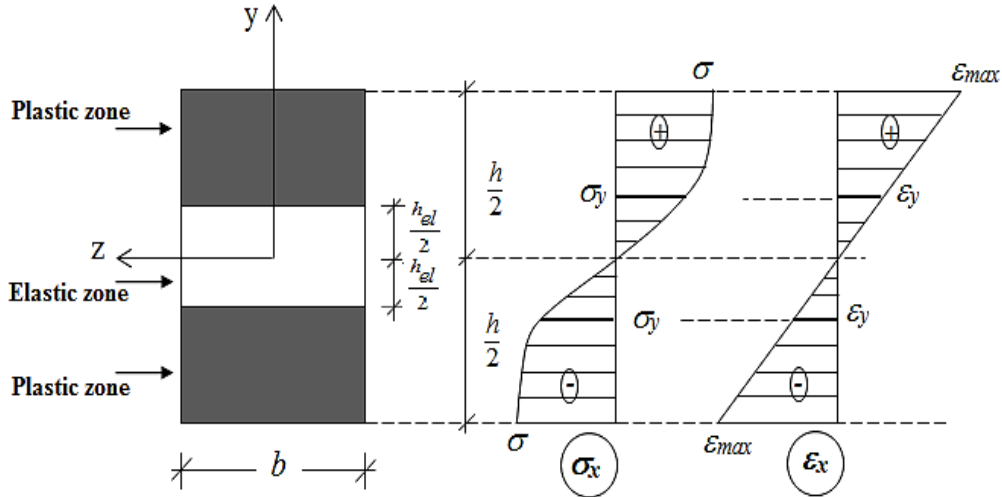


Figure 5. Elastic plastic stress and strain distribution in the cross-section AB

Effect of Peeling Angle

Figure 6 shows the variation of J-integral as a function of normalized crack length for different values of the peeling angle θ and $h_f/h_s = 0.075$. For $\theta < 45^\circ$ whatever a/w , the J parameter is nearly constant and this is mainly due to lower stress and strain fields at the interfacial crack tip. The effect of the peeling angle θ appears when its value exceeds 45° and a/w is above 0.12; a very large gap between the values of the J-integral is noted. In this case, the interfacial fracture energy increases rapidly. It reaches its maximum at a loading orientation of 90° . This may be due to the fact that the crack is solicted mainly in pure opening mode I. Then the strain and stress fields can be almost maximum resulting from the increase of the J parameter. When the angle θ decreases the crack propagates in mixed mode (I + II), with the dominance of the mode I until 60° (dominance mode I). Below 60° , the dominance of mode II is observed. This orientation leads to a distribution of normal and shearing stresses in the interface. This distribution gives mixed mode behaviour of the crack. The values of the J-integral do not present a risk of brutal fracture because they are largely lower than the toughness of the pair film/substrate. The results of Figure 6 show that the increase of the peeling angle θ leads to the increase of the J parameter and consequently to the expansion of the plastic zone size at the crack tip.

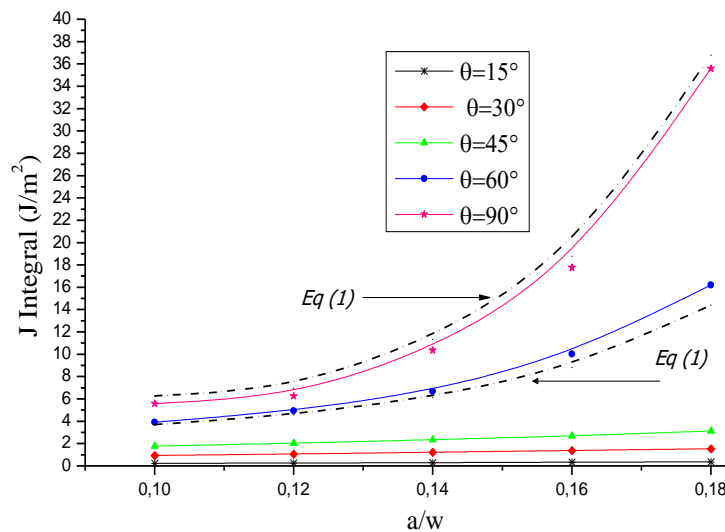


Figure 6. Variation of J integral vs a/w for different peeling angle θ ($h_f/h_s = 0.075$)

Figure 7 illustrates the extent of the plastic zone for different values of angle θ , ($a/w = 0.18$ and $h_f/h_s = 0.075$). The plastic zone depends strongly on the peeling angle θ . Indeed, the plastic zone size increases with the peeling angle. Thus, the plastic zone area for $\theta = 90^\circ$ is much greater compared to that for $\theta = 15^\circ$. This increase of the plastic zone can be due to a significant plastic strain caused by the increase of the peeling angle of film where the mode I dominates the mode II. For small angles, the plastic zone has a circular shape around the crack tip. However, when the opening of the film increases, the area of the plastic zone extends over the entire thickness of the film above the crack tip.

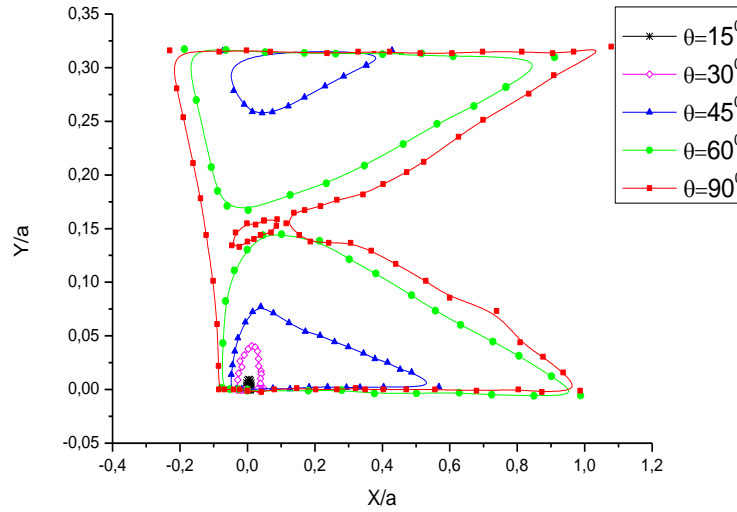


Figure 7. Contour of plastic zone for different peeling angle θ ($a/w = 0.18$)

Effect of Residual Stresses

To study the effect of residual stresses on the film-substrate system, the film/substrate composite is subjected to thermo-mechanical loading; the couple is heated to temperatures of elaboration and then cooled to room temperature (25°C). The film is subjected to a tensile load F . The film has an elastic plastic behaviour whose the stress-strain curve at different temperature is shown on Figure 8.

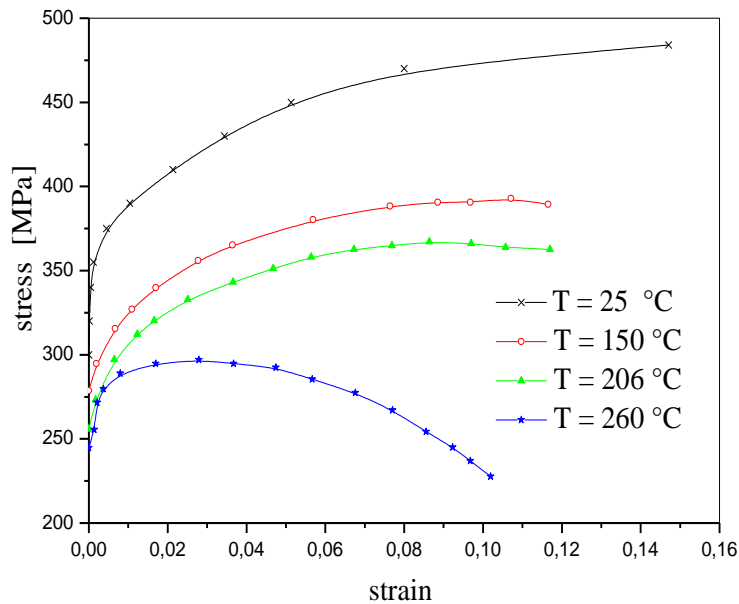


Figure 8. Stress-Strain curve of film at different temperature

Table 1 gives the mechanical and thermal properties of the film and substrate at different temperatures. The thermal residual stresses are created during cooling at room temperature. The differences between thermal and mechanical properties are the source of a heterogeneous strain between the two materials. A gradient of residual stress develops in the two materials in the vicinity of the interface. These developed residual stresses represent the initial state of stress field in both film and substrate prior to mechanical loading.

Table 1. Mechanical and thermal properties of the substrate and film at different temperatures

$T(^{\circ}\text{C})$	E_s (MPa)	E_f (MPa)	ν_s	ν_f	α_s ($1/^{\circ}\text{K}$)	α_f ($1/^{\circ}\text{K}$)
25	34500	7200	0.3	0.33	6.2×10^{-6}	2.26×10^{-6}
150	343100	68000	0.3	0.33	7×10^{-6}	2.26×10^{-6}
206	342800	63000	0.3	0.33	7.2×10^{-6}	2.30×10^{-6}
260	342000	59000	0.3	0.33	7.3×10^{-6}	2.33×10^{-6}

Figure 9 shows the variation of the J-integral as a function of normalized crack length a/w for different temperatures ΔT . The analysis of this figure clearly reflects that the rise of the temperature ΔT leads to an increase of the fracture energy at the interface crack. Indeed, the most significant values of the J-integral are obtained for high crack lengths, particularly above $a/w = 0.16$ and high temperature ΔT values. Thus, the mechanical properties of the metal ductility increases, involving an increase in plastic strain close to the vicinity of the crack, which is directly related to the J-integral value. Comparing J-integral values, it can be seen that the fracture energy value obtained for $\Delta T = 235^{\circ}\text{C}$ is worth almost double of that obtained at room temperature $\Delta T = 0^{\circ}\text{C}$.

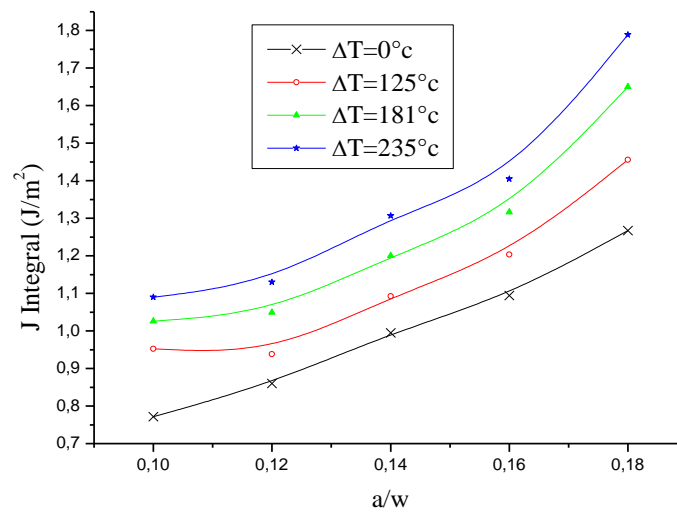


Figure 9. Variation of J integral vs a/w for different temperature ΔT ($h_f/h_s=0.075$, $\theta=30^{\circ}$)

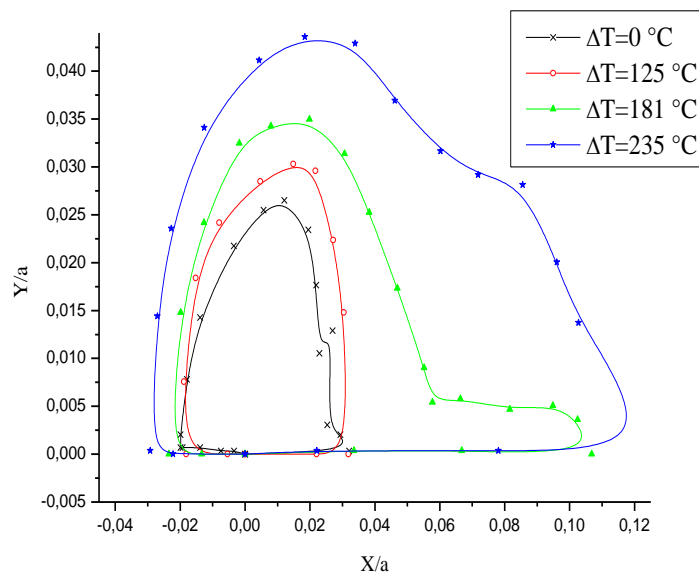


Figure 10. Variation Contour of plastic zone for different temperature ΔT ($a/w=0.18$, $h_f/h_s=0.075$, $\theta=30^{\circ}$)

The extent of plastic zone for different temperatures ΔT is shown in Figure 10, for a normalized crack length $a/w = 0.18$. The same phenomenon observed in Figure 9 is encountered in Figure 10. The size and shape of the plastic zone depends on the mechanical properties of ductility of metal. These properties vary upward with temperature creating a significant plasticization around the crack tip. Indeed, when the temperature increases, the plastic zone size is more expanding while approaching the crack tip. The area of the plastic zone obtained for $\Delta T = 235^\circ\text{C}$ is nearly twice of that obtained at $\Delta T = 0^\circ\text{C}$.

CONCLUSIONS

Peeling angle and residual stresses effects on the film-substrate system was numerically conducted and the results are summarized as below:

1. The J-integral values at interfacial crack tip depend on both the crack length, the peeling angle of the film debonded with respect to the substrate and the mechanical energy at the crack tip.
2. The opening effect of the peeling angle describes a threshold of 45° . When this angle decreases below this threshold, it can be seen the dominance of mode II fracture providing weak variation of J-integral value. Beyond 45° the fracture energy increases rapidly due to the fact that the crack is solicited towards mixed mode until 60° where fracture can occur. From 60° to 90° the dominance of mode I increases rapidly the J-integral value. In another hand, the gradual opening of the peeling angle generates an increasingly wide plastic zone around the crack tip to extend over the almost thickness of the film.
3. J-integral and plastic zone size parameters reach their maximum values when the film is oriented perpendicular to the substrate.
4. Delamination of thin film is highly dependent on thermal residual stresses. The increase in temperature leads to an intensified interfacial fracture energy and the extent of the plastic zone at the crack tip.

REFERENCES

- [1] T. Pardoën, T. Ferracin, C. M. Landis, F. Delannay, "Constraint effects in adhesive joint fracture," *J. Mech. Phys. Solids*, vol. 53, no. 9, pp. 1951–1983, 2005, doi: 10.1016/j.jmps.2005.04.009.
- [2] B. Cotterell, K. Hbaieb, J. G. Williams, H. Hadavinia, V. Tropsa, "The root rotation in double cantilever beam and peel tests," *Mech. Mater.*, vol. 38, no. 7, pp. 571–584, 2006, doi: 10.1016/j.mechmat.2005.11.001.
- [3] H. Hadavinia, L. Kawashita, A. J. Kinloch, D. R. Moore, J. G. Williams, "A numerical analysis of the elastic-plastic peel test," *Eng. Fract. Mech.*, vol. 73, no. 16, pp. 2324–2335, 2006, doi: 10.1016/j.engfracmech.2006.04.022.
- [4] F. Daghia, C. Cluzel, L. Hébrard, F. Churlaud, B. Courtemanche, "The Double Drum Peel (DDP) test: a new concept to evaluate the delamination fracture toughness of cylindrical laminates," *Compos. Part A Appl. Sci. Manuf.*, vol. 113, pp. 83–94, 2018, doi: 10.1016/j.compositesa.2018.07.020.
- [5] Y. Sekiguchi, A. A. Hayashi, C. Sato, "Analytical determination of adhesive layer deformation for adhesively bonded double cantilever beam test considering elastic-plastic deformation," *J. Adhes.*, vol. 96, no. 7, pp. 647–664, 2018, doi: 10.1080/00218464.2018.1489799.
- [6] S. Abdullah, M. F. Abdullah, W. N. M. Jamil, "Ballistic performance of the steel-aluminium metal laminate panel for armoured vehicle," *J. Mech. Eng. Sci.*, vol. 14, no. 1, pp. 6452–6460, 2020, doi: 10.15282/jmes.14.1.2020.20.0505.
- [7] E. Simlissi, M. Martiny, S. Mercier, S. Bahi, L. Bodin, "Elastic-plastic analysis of the peel test for ductile thin film presenting a saturation of the yield stress," *Int. J. Fract.*, vol. 220, no. 1, pp. 1–16, 2019, doi: 10.1007/s10704-019-00393-7.
- [8] J. Song, W. Y. Yueguang, "Trans-scale characterization of interface fracture in peel test for metal film/ceramic substrate systems," *Eng. Fract. Mech.*, vol. 221, no. 0013-7944, pp. 106679, 2019, doi: 10.1016/j.engfracmech.2019.106679.
- [9] M. S. Islam, K. S. Alfredsson, "Peeling of metal foil from a compliant substrate," *J. Adhes.*, pp. 1–32, 2019, doi: 10.1080/00218464.2019.1696678.
- [10] Y. Hong-hui, J. W. Hutchinson, "Delamination of thin film strips," *Thin Solid Films*, vol. 423, no. 1, pp. 54–63, 2003, doi: 10.1016/S0040-6090(02)00973-2.
- [11] P. H. Martiny, F. Lani, A. J. Kinloch, T. Pardoën, "Numerical analysis of the energy contributions in peel tests: A steady-state multilevel finite element approach," *Int. J. Adhes. Adhes.*, vol. 28, no. 4-5, pp. 222–236, 2008, doi: 10.1016/j.ijadhadh.2007.06.005.
- [12] Y. Wei, J. W. Hutchinson, "Nonlinear delamination mechanics for thin films," *J. Mech. Phys. Solids*, vol. 45, no. 7, pp. 1137–1159, 1997, doi: 10.1016/S0022-5096(96)00122-6.
- [13] V. Tvergaard, J. W. Hutchinson, "The relation between crack growth resistance and fracture process parameters in elastic-plastic solids," *J. Mech. Phys. Solids*, vol. 40, no. 6, pp. 1377–1397, 1992, doi: 10.1016/0022-5096(92)90020-3.
- [14] V. Tvergaard, J. W. Hutchinson, "The influence of plasticity on mixed mode interface toughness," *J. Mech. Phys. Solids*, vol. 41, no. 6, pp. 1119–1135, 1993, doi: 10.1016/0022-5096(93)90057-M.

- [15] Z. Suo, C. F. Shih, A. G. Varias, "A theory for cleavage cracking in the presence of plastic flow," *Acta Metall. Mater.*, vol. 40, no. 5, pp. 1551-1557, 1993, doi: 10.1016/0956-7151(93)90263-R.
- [16] Z. C. Leseman, S. P. Carlson, J. M. Thomas, "Experimental Measurements of the Strain Energy Release Rate for Stiction-Failed Microcantilevers Using a Single-Cantilever Beam Peel Test," *J. Microelectromech Syst.*, vol. 16, no. 1, pp. 38 – 43, 2007, doi: 10.1109/JMEMS.2006.883570.
- [17] J. A. Williams, J. J. Kauzlarich, "The influence of peel angle on the mechanics of peeling flexible adherends with arbitrary load–extension characteristics," *Tribol. Int.*, vol. 38, no. 11-12, pp. 951–958, 2005, doi: 10.1016/j.triboint.2005.07.024.
- [18] H. Zhao, Y. Wei, "Determination of interface properties between micron-thick metal film and ceramic substrate using peel test," *Int. J. Fract.*, vol. 144, pp. 103–112, 2007, doi: 10.1007/s10704-007-9083-4.
- [19] M. D. Thouless, Q. D. Yang, "A parametric study of the peel test," *Int. J. Adhes. Adhes.*, vol. 28, no. 4-5, pp. 176–184, 2008, doi: 10.1016/j.ijadhadh.2007.06.006.
- [20] P. Ghabezi, M. Farahani, "Characterization of cohesive model and bridging laws in mode I and II fracture in nanocomposite laminates," *J. Mech. Eng. Sci.*, vol. 12, no. 4, pp. 4329-4355, 2018, doi: 10.15282/jmes.12.4.2018.24.0370.
- [21] I. Georgiou, H. Hadavinia, A. Ivankovic, A. J. Kinloch, V. Tropsa, J. G. Williams, "Cohesive zone models and the plastically deforming peel test," *J. Adhes.*, vol. 79, no. 3, pp. 239-265, 2010, doi: 10.1080/00218460309555.
- [22] Z. Gan, S. G. Mhaisalkar, C. Zhong, Z. Sam, Z. Chen, K. Prasad, "Study of interfacial adhesion energy of multilayered ULSI thin film structures using four-point bending test," *Surf. Coat. Technol.*, vol. 198, no. 1-3, pp. 85–89, 2005, doi: 10.1016/j.surfcoat.2004.10.036.
- [23] P. J. J. Forschelen, A. S. J. Suiker, O. V. D. Sluis, "Effect of residual stress on the delamination response of film-substrate systems under bending," *Int. J. Solids Struct.*, vol. 97-98, no. 0020-7683, pp. 284-299, 2016, doi: 10.1016/j.ijsolstr.2016.07.020.
- [24] S. Chauffaille, J. Jumel, M. E. R. Shanahan, "Elasto-plastic analysis of the single cantilever beam adhesion test," *Eng. Fract. Mech.*, vol. 78, no. 13, pp. 2493–2504, 2011, doi: 10.1016/j.engfracmech.2011.06.009.
- [25] L. Zhang, J. Wang, "A generalized cohesive zone model of the peel test for pressure-sensitive adhesives," *Int. J. Adhes.*, vol. 29, no. 3, pp. 217–224, 2009, doi: 10.1016/j.ijadhadh.2008.05.002.
- [26] N. A. Fleck, J. W. Hutchinson, "Strain gradient plasticity," *Adv. Appl. Mech.*, vol. 33, pp. 295-361, 1997.
- [27] N. A. Fleck, J. W. Hutchinson, "A reformulation of strain gradient plasticity," *J. Mech. Phys. Solids*, vol. 49, no. 10, pp. 2245–2271, 2001, doi: 10.1016/S0022-5096(01)00049-7.
- [28] Z. Sun, W. Kai-Tak, D. A. Dillard, "A theoretical and numerical study of thin film delamination using the pull-off test," *Int. J. Solids Struct.*, vol. 41, no. 3-4, pp. 717–730, 2004, doi: 10.1016/j.ijsolstr.2003.09.027.
- [29] S. Guo, W. Kai-Tak, D. A. Dillard, "A bending-to-stretching analysis of the blister test in the presence of tensile residual stress," *Int. J. Solids Struct.*, vol. 42, no. 9-10, pp. 2771–2784, 2005, doi: 10.1016/j.ijsolstr.2004.10.007.
- [30] M. Zhan, X. Chen, J. Yan, A. M. Karlsson, "Determination of uniaxial residual stress and mechanical properties by instrumented indentation," *Acta Mater.*, vol. 54, no. 10, pp. 2823–2832, 2006, doi: 10.1016/j.actamat.2006.02.026.
- [31] J. Yan, A. M. Karlsson, X. Chen, "Determining plastic properties of a material with residual stress by using conical indentation," *Int. J. Solids Struct.*, vol. 44, no. 11-12, pp. 3720–3737, 2007, doi: 10.1016/j.ijsolstr.2006.10.017.
- [32] F. Gruttmann, V. D. Pham, "A finite element model for the analysis of buckling driven delaminations of thin films on rigid substrates," *Comput. Mech.*, vol. 41, no. 3, pp. 361–370, 2008, doi: 10.1007/s00466-007-0191-9.
- [33] O. Onen, D. Lynford, C. Nelson, O. G. Rasim, "Thermal stresses on membrane based microdevices," *Microsyst. Technol.*, vol. 16, no. 11, pp. 1967–1973, 2010, doi: 10.1007/s00542-010-1130-9.
- [34] S. Hibbitt, Karlsson. *ABAQUS Standard Version 6.9*, Dassault Systèmes Simulia Corp., Providence, RI, USA, 2009.
- [35] V. Rizov, "Non-linear fracture behavior of double cantilever beam," *Eng. Mech.*, vol. 22, no. 2, pp. 95-102, 2015, doi: 10.3233/SFC-150186.